Neuropharmacology 219 (2022) 109237

Contents lists available at ScienceDirect

Neuropharmacology

journal homepage: www.elsevier.com/locate/neuropharm

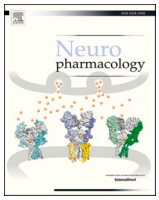

CREB serine 133 is necessary for spatial cognitive flexibility and long-term potentiation

Lorenzo Morè [a,2,1], Lucia Privitera [a,3,1], Philippa Perrett [a], Daniel D. Cooper [a], Manuel Van Gijsel Bonnello [b], J. Simon C. Arthur [b], Bruno G. Frenguelli [a,*]

[a] School of Life Sciences, University of Warwick, Coventry, CV4 7AL, UK
[b] Division of Cell Signalling and Immunology, Wellcome Trust Building, College of Life Sciences, University of Dundee, Dundee, DD1 5EH, UK

ARTICLE INFO

Keywords:
CREB
Cyclic AMP response element-binding protein
LTP
Learning and memory
Plasticity

ABSTRACT

The transcription factor cAMP response element-binding protein (CREB) is widely regarded as orchestrating the genomic response that underpins a range of physiological functions in the central nervous system, including learning and memory. Of the means by which CREB can be regulated, emphasis has been placed on the phosphorylation of a key serine residue, S133, in the CREB protein, which is required for CREB-mediated transcriptional activation in response to a variety of activity-dependent stimuli. Understanding the role of CREB S133 has been complicated by molecular genetic techniques relying on over-expression of either dominant negative or activating transgenes that may distort the physiological role of endogenous CREB. A more elegant recent approach targeting S133 in the endogenous CREB gene has yielded a mouse with constitutive replacement of this residue with alanine (S133A), but has generated results (no behavioural phenotype and no effect on gene transcription) at odds with contemporary views as to the role of CREB S133, and which may reflect compensatory changes associated with the constitutive mutation. To avoid this potential complication, we generated a post-natal and forebrain-specific CREB S133A mutant in which the expression of the mutation was under the control of CaMKIIα promoter. Using male and female mice we show that CREB S133 is necessary for spatial cognitive flexibility, the regulation of basal synaptic transmission, and for the expression of long-term potentiation (LTP) in hippocampal area CA1. These data point to the importance of CREB S133 in neuronal function, synaptic plasticity and cognition in the mammalian brain.

1. Introduction

The transcription factor cAMP response element-binding protein (CREB) has achieved widespread recognition for its role as a major mechanism by which gene expression is regulated in response to a wide range of physiological stimuli, and in initiating the transcriptional response that underpins learning and memory in an evolutionarily-conserved manner (Alberini and Kandel, 2014; Kida and Serita, 2014; Nonaka et al., 2014; Lisman et al., 2018).

The mechanisms by which CREB is regulated are complex, and involve, among other mechanisms, the phosphorylation of key serine residues on CREB. In particular, phosphorylation of serine 133 (S133) by a range of protein kinases including PKA, CaMKs, RSK and MSK1 has been implicated in regulating synaptic plasticity and learning and memory (Johannessen et al., 2004; Flavell and Greenberg, 2008; Barco and Marie, 2011; Reyskens and Arthur, 2016; Belgacem and Borodinsky, 2017; Daumas et al., 2017; Privitera et al., 2020). Indeed, restoring or enhancing phosphorylation of CREB S133 may be a major contributor to the cognition-enhancing effects of phosphodiesterase inhibitors and related compounds additionally targeting acetylcholinesterase (Mao et al., 2018; Ni et al., 2018). Such compounds are currently being developed for the treatment of Alzheimer's disease and other neurological and psychiatric disorders (Zuccarello et al., 2020).

It is against this backdrop that a study with a mouse expressing a

* Corresponding author.
E-mail address: b.g.frenguelli@warwick.ac.uk (B.G. Frenguelli).
[1] These authors contributed equally to this study.
[2] present address: School of Pharmacy and Biomedical Sciences, University of Central Lancashire, Preston PR1 2HE, UK.
[3] present address: Barts and the London School of Medicine, Queen Mary University of London Malta Campus Victoria Triq L-Arċisqof Pietru Pace, Victoria, VCT 2570.

https://doi.org/10.1016/j.neuropharm.2022.109237
Received 13 May 2022; Received in revised form 18 August 2022; Accepted 23 August 2022
Available online 30 August 2022

constitutive mutation of the CREB gene, in which S133 is converted to an alanine (CREB S133A), has yielded results that challenge this view (Briand et al., 2015). This mutant mouse displayed no deficit in hippocampus/amygdala-dependent contextual or cued fear conditioning, or striatum-dependent instrumental learning. Surprisingly, no deficits in gene induction were observed under either basal conditions or in response to fear conditioning, nor in the binding of CREB to DNA. This was not explained by increases in two related transcription factors, CREM and ICER, which remained at levels found in wild-type animals.

These observations are at odds with a previous study from our laboratory (Wingate et al., 2009): using a conditional knock-in point mutation of the endogenous CREB gene that also generated a CREB S133 to alanine mutation (S133A), deficits in gene induction were observed in cultured cortical neurons prepared from mice in which the mutation was under the control of the nestin promoter. Using this model, CREB S133 phosphorylation has also been shown to affect gene induction in fibroblasts and macrophages (Elcombe et al., 2013; Naqvi et al., 2014) indicative of the widespread role of this residue in regulating gene expression.

We have now extended these observations by placing the conditional CREB S133A mutation under the control of the CaMKIIα promoter (Minichiello et al., 1999). This has allowed us to generate mice with post-natal and forebrain-specific substitution of CREB S133 with alanine. Mice with the CREB S133A mutation displayed deficits in spatial cognitive flexibility, basal synaptic transmission and long-term potentiation. These results demonstrate the importance of CREB S133 in the regulation of synaptic plasticity and cognition in the mammalian brain.

2. Methods

2.1. Animals

The conditional mutation in exon 5 of the Creb1 gene, which codes for S133 and is common to all three isoforms of CREB, is described in Wingate et al. (2009). This mouse line, on a C57BL/6J background, was crossed with a mouse line, also on a C57BL/6J background, expressing the Tg(Camk2a-cre)159Kln CaMKIIα promoter (Minichiello et al., 1999) to generate mice in which Cre-mediated excision of the floxed wild-type S133 results in the expression of the CREB S133A mutant protein after approximately post-natal day 20 and in a forebrain-specific manner (neocortex, hippocampus, amygdala). In the present study $Cre^{+}CREB^{+/+}$ (CREB Control) and Cre $^{+}$ $CREB^{fl/fl}$ (CREB S133A) mice were used to control for the expression of Cre recombinase.

2.2. Western blotting

Western blots were prepared from hippocampal slices taken from CREB Control and CREB S133A mice of ~3 months of age. The tissue was homogenised in lysis buffer containing: 50 mM Tris-HCl, pH 7.5, 1% TritonX-100, 0.1% SDS, 1 mM Na_3VO_4, 50 mM NaF, 5 mM $Na_4P_2O_7$,0.27 M sucrose, 0.02% NaN_3, and protease inhibitor mixture tablets (Roche). Samples were aliquoted out to equal concentrations, mixed with loading buffer (7.5 mM trisHCl pH 6.8, 25% glycerol, 2% SDS, 0.01% bromophenol blue) in a 2:1 ratio of sample to loading buffer, and stored at −20 °C until required for western blotting. After defrosting, samples were brought to 80 °C for 5 min, spun briefly and the proteins were separated using SDS-PAGE electrophoresis in a 15% polyacrylamide gel. After separation, proteins were transferred onto nitrocellulose blotting membrane (GE Healthcare) in a semi-wet system for 2.5 h at 200 mA. The membrane was blocked in 10% Marvel milk powder and 0.5% TWEEN in phosphate-buffered saline (PBS) for 1 h. Membranes were incubated in a primary antibody against GAPDH (CST 2118s) in 1% Marvel milk powder in 0.05% PBS TWEEN (PBS-T) solution for 2 h at room temperature (RT), followed by the washing protocol, consisting of four 10 min washes in 0.1% PBS-T. Samples were incubated overnight at 4 °C with a second primary antibody recognizing phospho-S133 CREB (#9198, 1:500), from Cell Signalling Technology, and then washed with the same protocol as before. Membranes were incubated for 1–2 h in horseradish peroxidase-conjugated anti-rabbit antibody (1:10,000 dilution, ThermoFisher #31460). After washing as previously described, membranes were incubated for 2 min in Clarity Western ECL reagent (BioRad) and imaged using the ImageQuant LAS 4000 CCD Biomolecular Imager. Image Studio Lite V 5.2.5 was used to analyse the signal of the bands, and the protein of interest was normalised to the control protein analysed. After stripping the membrane (Re-blot Plus Mild Antibody Stripping solution, EMD millipore), Membranes were reblocked and incubated in total CREB (#9197, 1:1000; from Cell Signalling Technology), overnight at 4° and followed the same protocol as above.

2.3. Immunofluorescence

The immunofluorescence methods for pCREB have been described previously (Daumas et al., 2017). Hippocampal slices (400 μm from 7 to 10 month old male mice) were fixed overnight in paraformaldehyde (4% in PBS, pH 7.4) The slices were washed three times in PBS and then incubated for 1.5 h at room temperature in a solution consisting of 0.4% Triton X-100 in PBS and 10% goat serum. After three subsequent washes in PBS the slices were incubated for 4 h at room temperature with a phospho-CREB primary antibody targeting S133 (rabbit mAb; Cell Signalling; #9198; 1:400 in 10% donor goat serum and 0.4% Triton X-100 in PBS). After two washes in PBS, slices were incubated for 1.5 h at room temperature in Alexa Fluor 488 goat anti-rabbit antibody (Molecular Probes; #A-11008; 1:800 in 10% donor goat serum and 0.4% Triton X-100 in PBS). The slices were then washed again in PBS three times before being mounted in a medium containing DAPI to stain cell nuclei (Fluoroshield™ with DAPI; Sigma, #F6057). The slices were viewed, and images were acquired blind to the genotype using identical settings with Zeiss ZEN2 software on an LSM 880 laser confocal-scanning system coupled to a Zeiss inverted microscope. Images were taken using a 40 x oil immersion objective. Quantification of the size of DAPI-stained nuclei involved threshold-defining DAPI staining against background and considering only whole nuclei from maximum intensity projections of image z-stacks (Supplementary Fig. 1). The number of pixels within the boundary of the identified nuclei was recorded.

2.4. RNA expression

Total RNA was isolated from ~3 month old male mice using RNeasy kits (Qiagen) and then reverse transcription carried out using iScript according to the manufacturer's instructions. The levels of CREB, ATF1, ICER and CREM were determined by qPCR using sybergreen-based detection (Takara). Primer sequences are listed in Table 1. Levels were calculated relative to the average of GAPDH and 18S mRNA levels using the equation expression = 2^(Ct(Ave GAPDH / 18s)-Ct(CREB family mRNA)).

2.5. Behaviour

$Cre^{+}CREB^{+/+}$ (CREB Control; n = 14, 6 males/8 females) mice were compared to Cre $^{+}$ $CREB^{fl/fl}$ (CREB S133A; n = 10, 6 males and 4 females) mice. Both male and female mice of 2.5–5 months of age were used. Open field ± novel object, elevated plus maze, spontaneous alternation and serial spatial learning tasks were adapted from those reported in previous studies (Chen et al., 2000; D'Adamo et al., 2014; Oettinghaus et al., 2016; Pennucci et al., 2016; Daumas et al., 2017; Privitera et al., 2020).

2.5.1. Neurological assessment

Assessment of neurological parameters was performed at P60 and was adapted from (Wolf et al., 1996). Mice were scored with 1 point for each neurological sign observed and 0 scores a fully healthy subject. All

Table 1
Primer sequences used for qPCR.

gene	Sense	antisense
ICER	CCAAAGCATGGGCAGCAAAAGTG	GCAATTGTTGCTACCTGAACAGTTTG
CREB	CCATGGAATCTGGAGCAGACAACC	GGACTTGTGGAGACTGGATAACTGATGG
CREM	GGAAAACAGGGAAGGAACAAAGCATTG	GCTACAGAAACCTGAGCTAGAGTAGG
ATF1	GGAAGATTCCCACAAGAGTAACACGAC	GGTCTTTCAAAATTTTCCTGTAGGATGGG
GAPDH	GTAACCCGTTGAACCCCATT	CCATCCAATCGGTAGTAGCG
18S	ACAGTTCTTATGTGGTGACCC	TGCACCACCAACTGCTTAG

mice scored 0 points.

2.5.2. Spontaneous alternation

A standard 8 arm radial maze for mice (Ugo Basile) was placed inside the empty water maze tank and four out of the eight arms (with walls) were kept open to form a plus shape (+). Each mouse was individually released in the centre of the maze and tracked for 10 min. The sequence of arm entries was scored. A correct alternation was considered when a mouse made only one repetition in 5 entries (Oettinghaus et al., 2016; Pennucci et al., 2016).

2.5.3. Elevated plus-maze

A standard 8 arm radial maze for mice (Ugo Basile) was placed inside the empty water maze tank and raised 60 cm from the tank base. Four out of the eight arms were kept open to form a plus shape (+); two of the arms had walls while the other two (opposite one another) lacked walls. Each mouse was individually released in the centre of the maze and tracked for 10 min.

2.5.4. Open field and novel object task

These tests were run as two consecutive stages of the same experiment. Four open field boxes (Ugo Basile; 44 × 44 × 44 cm) were placed inside the empty water maze tank to form a square and 4 mice were tested simultaneously. Each mouse was singly released in the box and tracked. The open field lasted 1 h, after which a 50-ml Falcon vial (novel object) was attached upside-down to the centre of the open field and the mouse was tracked for an additional hour.

2.5.5. Water maze serial spatial learning

Stage 1 Habituation (day 1): each mouse was placed on a 20 cm diameter platform located in the centre of a 180 cm diameter pool filled with opaque water (27 °C) and was allowed to observe the environment for 2 min. The pool was surrounded by curtains which did not allow the distal visual cues to be seen. Water level was ca. 1 cm above the platform. Each mouse then received 3 consecutive trials (different starting points) where it was left free to swim in the pool for a maximum of 90 s and then placed on the platform and left there for 30 s.

Stage 2 Visual Cue (day 2): The platform was placed in the centre of the pool and an object was placed upon it (yellow TV plastic toy 6 × 6 × 5 cm). Each mouse received 4 trials (different cardinal starting points) where it was left free to swim in the pool for a maximum of 90 s. Water level was ca. 1 cm above the platform, with the water in the pool maintained at 26 °C. The pool was surrounded by curtains which did not allow the distal visual cues to be seen.

Stage 3–7 (Spatial Problem (SP) 1 to 5): Curtains were removed. Water was kept at 26 °C. The platform was placed in 5 different positions (consecutively): South-East (SP1 inner circle), North (SP2 external circle), South-West (SP3 inner circle), East (SP4 external circle) and North-West (SP5 inner circle). Water level was ca. 1 cm above the platform. Each mouse received a maximum of 6 trials per day (4 different starting points) where it was left free to swim in the pool for max 60 s and then left on the platform for 20 s. There was a maximum of 18 trials per SP, i.e. 3 consecutive days of training. A given SP was considered completed when a mouse reached the platform in ≤30.0 s in three consecutive trials in a given day. When a subject completed one SP it was assigned to the following SP the next day. The inter-trial interval was approximately 4 min.

2.6. Electrophysiology

Dual pathway recordings of field excitatory postsynaptic potentials (fEPSPs) were made from area CA1 from hippocampal slices maintained in an interface chamber and taken from male mice (9–10 months of age) as described previously (Daumas et al., 2017; Privitera et al., 2020). In brief, fEPSP input/output curves extended over the stimulus range of 20–300 μA; paired-pulse facilitation over 15–350 ms inter-pulse interval, and long-term potentiation (LTP) was induced in response to theta-burst stimulation (TBS). Bursts consisted of 4 stimuli at 100 Hz; each train was composed of 10 bursts separated by 200 ms; trains were repeated 3 times with an interval of 20 s. Basal fEPSPs were set at 3 mV in amplitude to compensate for differences in basal synaptic transmission between CREB Control and CREB S133A mice. We have previously shown that LTP induced by TBS is sensitive to the transcription inhibitor actinomycin D (Daumas et al., 2017).

2.7. Statistics

Statistical analysis was performed using IBM SPSS 28. One and Two-way Univariate or Multivariate ANOVAs and RM-ANOVAs were performed as appropriate and as reported in the figure legends and statistical table. A post-hoc analysis was performed after each significant interaction via the Estimated Marginal Means with Sidak's correction. Statistical significance was accepted when $p < 0.05$. Data are presented as mean ± SEM. All experiments were conducted blind to genotype.

3. Results

3.1. Confirmation of the loss of CREB S133

To confirm the loss of CREB S133 in mice with the CREB S133A knock-in mutation we performed immunohistochemistry and western blotting from hippocampal slices prepared from CREB Control and CREB S133A mice. Immunohistochemistry with a monoclonal antibody directed at phosphorylated (p) CREB S133 showed abundant staining in the CA1 region in CREB Control mice (Fig. 1A). In contrast, no such staining was observed in the CA1 region of hippocampal slices taken from CREB S133A mice (Fig. 1B), despite there being a comparable number of CA1 pyramidal cells as indicated using the nuclear stain DAPI. DAPI staining revealed a potential difference in the size of the nuclei between the genotypes. A comparison of the size of DAPI-stained nuclei for CREB Control and CREB S133A mutant slices revealed that the DAPI-stained area of CA1 pyramidal cells in CREB S133A mutant slices were on average 12% smaller those in Control CA1 pyramidal cells (Supplementary Fig. 1). The reason for this difference is unclear, but may involve changes in the size of the nucleus, or state of the DNA, to which DAPI binds, between the two genotypes.

Western blotting confirmed the absence of pS133-CREB in the CREB mutants, but revealed similar levels of total CREB (Fig. 1C and Supplementary Fig. 2 with a longer exposure image). A qPCR analysis for CREB-related transcription factors in hippocampal tissue taken from

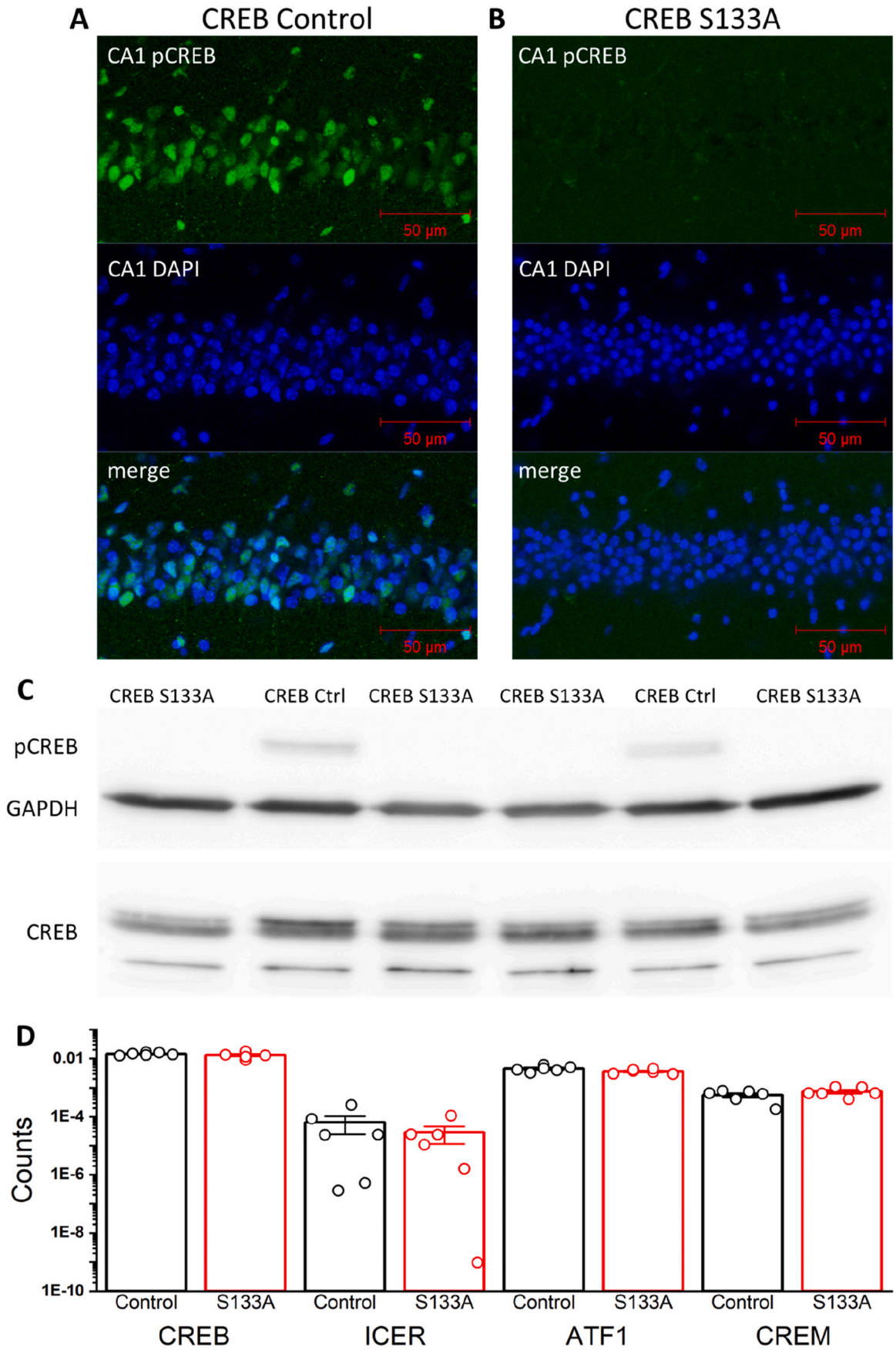

(caption on next page)

Fig. 1. The conditional CaMKIIα-driven CREB S133A mutation resulted in the loss of hippocampal CREB S133. A) Phosphorylated CREB S133 (pCREB) was expressed in CA1 pyramidal neurons from CREB Control mice, but not in CA1 pyramidal neurons from CREB S133A mutant mice (B), despite the presence of DAPI-labelled CA1 neurons. An analysis of DAPI staining can be found in Supplementary Fig. 1. Scale bar measures 50 μm. C) Western blotting in hippocampal slices from mice of either genotype confirmed the absence of pS133-CREB in CREB S133A mutant mice, but indicated comparable levels of total CREB between CREB Control and CREB S133A mutant mice (total CREB/GAPDH ratio of 0.920 and 0.916, respectively). GAPDH served as a loading control for comparable amounts of protein in each lane. An additional non-specific band was observed with the total CREB antibody at around 40 kDa. Full, untruncated blots with the molecular weight ladder can be found in Supplementary Fig. 3. D) qPCR analysis of hippocampal tissue showed comparable levels of mRNA expression of the transcription factors CREB, ICER, ATF1 and CREM. Data are presented as mean ± SEM with individual data points shown on the bar graphs.

CREB Control and CREB S133A mutant mice showed no difference in the RNA expression of CREB, ICER, ATF1 or CREM (Fig. 1D). This indicates that the loss of S133 phosphorylation of CREB was not compensated for by changes in the expression of other transcription factors.

3.2. CREB S133A mutant mice are impaired in spatial cognitive flexibility

To assess basal levels of locomotor and anxiety-like behaviour in CREB Control and CREB S133A mice, we subjected both genotypes to the open field-novel object and the elevated plus maze. In the open field CREB S133A mice consistently travelled further during the 2 h of the test, both before and after the introduction of a novel object after 60 min of the test (Fig. 2A). However, this difference did not reach statistical significance. In further analyses of behaviour in the open field-novel object test, including average speed, total distance travelled, resting time, latency to approach the novel object and time sniffing the novel object, we found no difference between the two genotypes, and nor were there any sex difference (Table 2).

In the elevated plus maze both genotypes displayed avoidance of the open area and there was no difference between the mice in terms of time spent on the open arms, nor in the distance travelled in the open arms, nor between males and females (Fig. 2B; Table 2). Thus, the loss of CREB S133 does not influence behaviour on these measures of locomotion, neophobia and anxiety-like behaviour.

To begin to test higher cognitive function, we assessed both CREB Control and CREB S133A mutant mice in spontaneous alternation behaviour, a test for hippocampus-dependent spatial working memory (Morè et al., 2007; Privitera et al., 2020). Both genotypes made comparable numbers of visits and entries into the open arms of a four-arm maze, although females made more entries than males (Table 2). Importantly, in terms of cognitive performance, both genotypes made similar levels of correct alternations between the open arms regardless of sex (Fig. 2C, Table 2). Thus, the CREB S133A mutation does not influence spatial working memory as assessed by the spontaneous alternation task.

Given the lack of a phenotype in the three previous tests, and the spatially- and temporally-restricted nature of the mutation, we performed a more challenging behavioural assessment involving the sequential learning of multiple platform locations in the water maze using visual cues external to the maze. There was no difference between CREB S133A and CREB Control mice in navigating to the submerged platform when clearly identified by a visible visual cue placed on the platform (Table 2), nor in finding the first spatial location of the hidden platform (Spatial Problem 1, SP1; Fig. 3A), which was true for both males and females (Fig. 3B and C). This suggests that the CREB S133A mutant mice have no gross motor, sensory or spatial reference memory impairment in a simple spatial task. However, performance in learning subsequent spatial locations, where interference from the acquisition of the previous spatial locations was maximized, was impaired. Overall, when male and female mice were combined, the CREB S133A mutant mice performed significantly worse than the CREB Control mice across the five training locations (Fig. 3A; Table 2). Despite evidence of a performance deficit in male mice (Fig. 3B), a statistically-significant impairment was only observed in female mice Fig. 3C; Table 2). These data indicate the need for CREB S133A for cognitive flexibility associated with spatial reference memory.

3.3. CREB S133 is required for the regulation of basal synaptic transmission and LTP in area CA1

Basal synaptic transmission was impaired in CREB S133A mutant mice (Fig. 4A): input-output curves of fEPSP slope *vs.* the amplitude of the presynaptic fibre volley showed a progressive increase in fEPSP slope in CREB Control mice that was not matched in the CREB S133A mice. A comparison of fEPSP slope and the fibre volley as a function of stimulus strength showed a significant deficit in the fEPSP slope, but no difference in fibre volley amplitude between the two genotypes (Fig. 4B). This latter observation suggests that the recruitment of presynaptic fibres was similar between mutant and control slices and could not explain the deficit in synaptic transmission. Similarly, the deficit in basal synaptic transmission was not caused by a reduction in the probability of glutamate release since the paired-pulse facilitation profile was similar between CREB Control and CREB S133A slices (Fig. 4C).

In order to test whether the CREB S133A mutation affected LTP, we performed dual pathway, theta-burst stimulation (TBS) in both CREB mutant and control slices. To compensate for differences in basal synaptic transmission between CREB S133A and CREB Control mice that may have influenced the induction of LTP, the amplitude of baseline fEPSPs was set at ~3 mV across genotypes. Robust and long-lasting (>90 min) LTP was induced in CREB Control slices (Fig. 4D). In contrast, LTP in CREB S133A mutant mice decayed to baseline within 80–90 min of LTP induction. These data reveal the importance of CREB S133 in the regulation of basal synaptic transmission, LTP and spatial cognitive flexibility.

4. Discussion

Using a conditional CREB S133A knock-in mutation of the endogenous CREB gene, we have avoided potential complications associated with either over-expression of exogenous CREB-targeting transgenes or constitutive mutations of CREB. We previously used this conditional mutant, under the control of the Nestin promoter to induce neuronal expression of the CREBS133A mutation, to investigate gene expression regulated by CREB S133 in primary cortical neurons (Wingate et al., 2009; Hunter et al., 2017). While there were no changes in the basal mRNA levels of CREB, CREM and ATF1 in the mutant neurons, the induction of CREB-dependent genes mkp-1 and nur77 in response to forskolin or BDNF was reduced in CREB S133A neurons (Wingate et al., 2009; Hunter et al., 2017).

To extend these observations to study the role of CREB S133 in synaptic plasticity and learning and memory, we chose to induce the S133A mutation was under the control of the CaMKIIα promoter, which gives rise to a post-natal and forebrain-specific pattern of CaMKIIα expression. While we did not perform a temporal analysis of post-natal S133A expression, the CRE mouse line we used (Tg(Camk2a-cre) 159Kln) (Minichiello et al., 1999) has been used extensively to induce selective post-natal gene induction commencing at 2–3 weeks, and variously confirmed by PCR, western blots and immunocytochemistry (Rios et al., 2001; Tolson et al., 2010; Bianchi et al., 2012; Stilling et al., 2014; Kaneko et al., 2016; Wickham et al., 2019; Di Domenico et al., 2021).

Comparable with observations made previously (Wingate et al., 2009; Hunter et al., 2017), the CaMKIIα-Cre-mediated loss of CREB S133 did not affect mRNA levels of the transcription factors CREB, CREM,

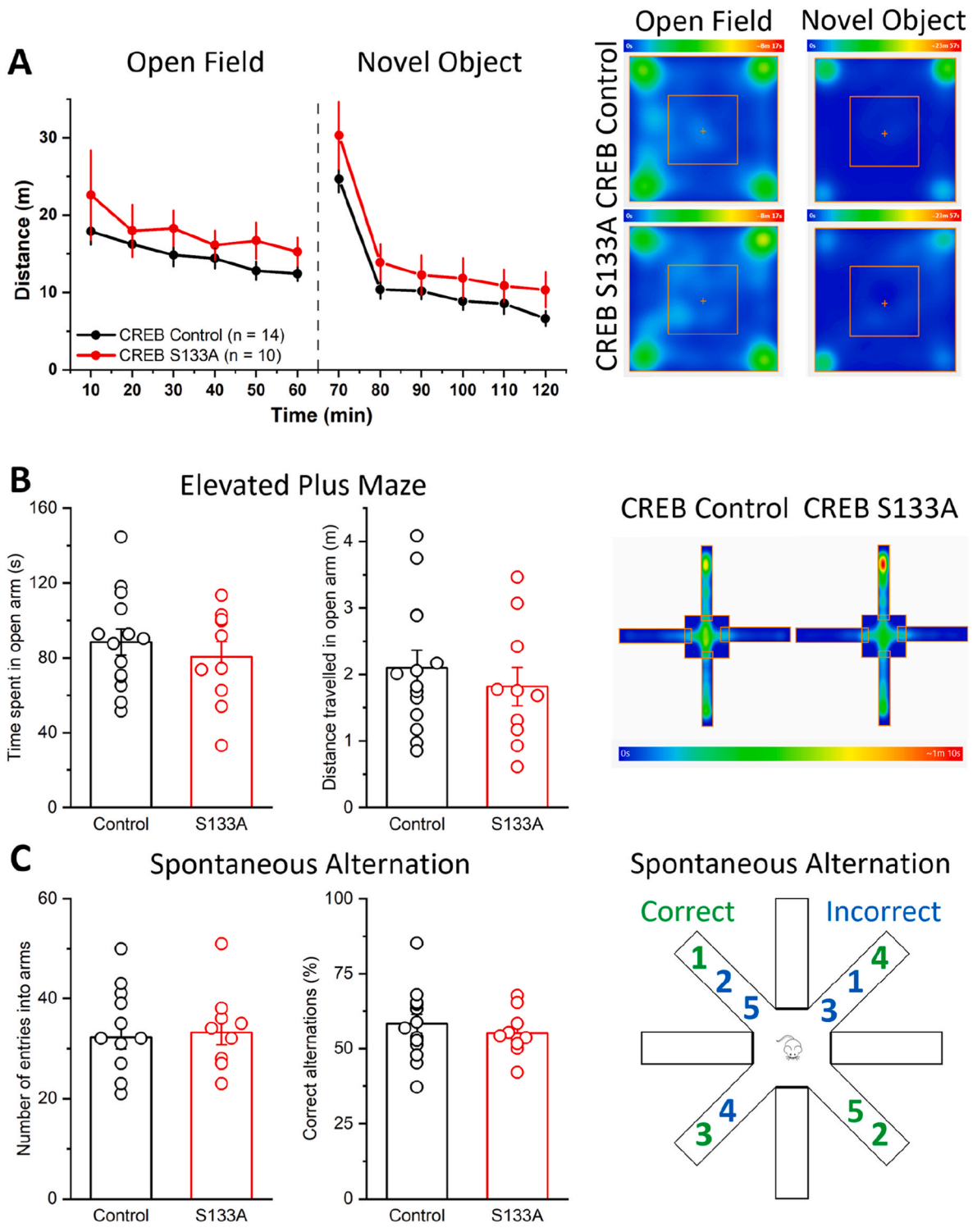

Fig. 2. Lack of gross sensorimotor, affective and spatial working memory deficits in the CREB S133A mutant mice. A) Locomotor activity in the open field and the response to the introduction of a novel object (dashed vertical line) were no different between CREB Control (black lines and symbols) and CREB S133A mice (red lines and symbols; $F_{1,22} = 1.30$, p: 0.270 and $F_{1,22} = 1.98$, p: 0.170, respectively). The inset heat maps show activity in the open field (0–60 min; left two heat maps) and after the introduction of the novel object (70–120 min; right two heat maps) in both CREB Control (upper two heat maps) and CREB S133A mice (lower two heat maps). B) CREB Control (black bars) and S133A mutant mice (red bars) spent comparable amounts of time (left bars) and travelled similar distances (right bars) in the open area of the elevated plus maze ($t_{22} = 0.730$, p: 0.470 and $t_{22} = 0.72$, p: 0.480, respectively). The inset heat maps show aggregate activity in the elevated plus maze for CREB Control (left) and CREB S133A mutant mice (right). Closed arms are shown vertically. C) There was no significant difference in the number of arm entries (left bars; $t_{22} = -0.29$, p: 0.770) nor in the percentage of correct alternations in the spontaneous alternation task for spatial working memory (right bars; $t_{22} = 0.72$, p: 0.480) between the genotypes. The inset shows the experimental set up and the criterion for correct (green) and incorrect (blue) alternations. Data are presented as mean ± SEM with individual data points shown on the bar graphs. Further statistical analysis is provided in Table 2.

Table 2
Statistical analysis of behavioural assays.

Test	Behavioural measure	With Sex as one independent variable.	Males only	Females only
Open Field-Novel Object	Latency to approach object (s)	Nobj: Genotype; F (1,20) = 1.41, p: 0.249. Sex; F (1,20) = 0.44, p: 0.513. Genotype x Sex; F (1,20) = 0.02, p: 0.905.	Nobj: Genotype; F (1,20) = 0.91, p: 0.351.	Nobj: Genotype; F (1,20) = 0.54, p: 0.472.
	Head in proximity of object (s)	Nobj: Genotype; F (1,20) = 0.18, p: 0.678. Sex; F (1,20) = 0.60, p: 0.448. Genotype x Sex; F (1,20) = 0.79, p: 384.	Nobj: Genotype; F (1,20) = 0.12, p: 0.736.	Nobj: Genotype; F (1,20) = 0.81, p: 0.378.
	Distance travelled (m)	OF: Genotype; F (1,20) = 0.78, p: 0.388. Sex; F (1,20) = 1.61, p: 0.219. Genotype x Sex; F (1,20) = 0.17, p: 6.88. Nobj: Genotype; F (1,20) = 1.50, p: 0.235. Sex; F (1,20) = 0.32, p: 0.579. Genotype x Sex; F (1,20) = 0.36, p: 0.553.	OF: Genotype; F (1,20) = 0.88, p: 0.359. Nobj: Genotype; F (1,20) = 1.78, p: 0.198.	OF: Genotype; F (1,20) = 0.11, p: 0.748. Nobj: Genotype; F (1,20) = 0.18, p: 0.674.
	Average speed (m/s)	OF: Genotype; F (1,20) = 0.78, p: 387. Sex; F (1,20) = 1.65, p: 0.214. Genotype x Sex; F (1,20) = 0.18, p: 0.678. Nobj: Genotype; F (1,20) = 1.43, p: 0.246 Sex; F (1,20) = 0.33, p: 573. Genotype x Sex; F (1,20) = 0.43, p: 0.521.	OF: Genotype; F (1,20) = 0.91, p: 0.353. Nobj: Genotype; F (1,20) = 1.81, p: 0.193.	OF: Genotype; F (1,20) = 0.10, p: 0.754. Nobj: Genotype; F (1,20) = 0.14, p: 0.713.
	Resting time (s)	OF: Genotype; F (1,20) = 0.12, p: 0.731. Sex; F (1,20) = 2.24, p: 0.150. Genotype x Sex; F (1,20) = 0.02, p: 0.883. Nobj: Genotype; F (1,20) = 1.26, p: 0.274. Sex; F (1,20) = 1.07, p: 0.313. Genotype x Sex; F (1,20) = 0.26, p: 0.614.	OF: Genotype; F (1,20) = 0.13, p: 0.720. Nobj: Genotype; F (1,20) = 1.42, p: 0.247.	OF: Genotype; F (1,20) = 0.19, p: 0.892. Nobj: Genotype; F (1,20) = 0.18, p: 0.679.
Elevated Plus Maze	Distance travelled (m)	Genotype; F (1,20) = 0.32, p: 0.577. Sex; F (1,20) = 0.37, p: 0.548. Genotype x Sex; F (1,20) = 1.13, p: 0.301.	Genotype; F (1,20) = 1.41, p: 0.249.	Genotype; F (1,20) = 0.12, p: 0.738.
	Average speed (m/s)	Genotype; F (1,20) = 0.39, p: 0.539. Sex; F (1,20) = 0.34, p: 0.564. Genotype x Sex; F (1,20) = 1.20, p: 0.287.	Genotype; F (1,20) = 1.57, p: 0.225.	Genotype; F (1,20) = 0.10, p: 0.751.
	Open arms time (s)	Genotype; F (1,20) = 0.41, p: 0.530. Sex; F (1,20) = 0.11, p: 0.745. Genotype x Sex; F (1,20) = 0.02, p: 0.899.	Genotype; F (1,20) = 0.13, p: 0.721.	Genotype; F (1,20) = 0.29, p: 0.598.
	Open arms distance travelled (m)	Genotype; F (1,20) = 0.19, p: 0.671. Sex; F (1,20) = 2.99, p: 0.099. Genotype x Sex; F (1,20) = 0.00, p: 0.999.	Genotype; F (1,20) = 0.10, p: 0.757.	Genotype; F (1,20) = 0.09, p: 0.770.
	Closed arms time (s)	Genotype; F (1,20) = 2.99, p: 0.099. Sex; F (1,20) = 0.82, p: 0.376. Genotype x Sex; F (1,20) = 0.23, p: 0.639.	Genotype; F (1,20) = 2.58, p: 0.124.	Genotype; F (1,20) = 0.74, p: 0.400.
	Closed arms distance travelled (m)	Genotype; F (1,20) = 1.33, p: 0.262. Sex; F (1,20) = 0.07, p: 0.794. Genotype x Sex; F (1,20) = 1.73, p: 0.204.	Genotype; F (1,20) = 3.24, p: 0.087.	Genotype; F (1,20) = 0.01, p: 0.914.
Spontaneous Alternation	Arm entries (#)	Genotype; F (1,20) = 1.11, p: 0.305. **Sex; F(1,20) = 16.30, p: 6.44 x 10^{-4}.** Genotype x Sex; F (1,20) = 0.15, p: 0.699. **Control, effect of sex F(1,20) = 5.67, p: 0.003 (F > M).** **S133A, effect of sex F(1,20) = 3.02, p: 0.028 (F > M).**	Genotype; F (1,20) = 1.11, p: 0.305.	Genotype; F (1,20) = 0.21, p: 0.655.
	Correct alternations (%)	Genotype; F (1,20) = 0.46, p: 0.507. Sex; F (1,20) = 0.01, p: 0.965. Genotype x Sex; F (1,20) = 0.59, p: 0.452.	Genotype; F (1,20) = 1.11, p: 0.305.	Genotype; F (1,20) = 0.01, p: 0.950.
Serial Spatial Learning	Visual Cue, average latency of all trials (s)	Genotype; F (1,20) = 0.03, p: 0.869. Sex: F (1,20) = 0.73, p: 0.402. Genotype x Sex; F (1,20) = 0.06, p: 0.816.	Genotype; F (1,20) = 0.03, p: 0.960.	Genotype; F (1,20) = 0.08, p: 0.785.
	Spatial problems solution; Trials to criterion (#)	**Spatial Problem effect: F(4,80) = 2.77 p: 0.033.** Spatial Problem × Sex interaction: F (4,80) = 0.99, p: 0.419. Spatial Problem x Genotype × Sex interaction: F (4,80) = 1.55, p: 0.196. **Genotype effect: F(1,20) = 7.40, p: 0.013.** Sex effect: F (1,20) = 0.45, p: 0.510. Genotype × Sex interaction: F (1,20) = 0.007, p: 0.933.	**Spatial Problem: F (4,40) = 4.06, p: 0.007.** SP x Genotype; F (4.40) = 1.55, p: 0.206. Genotype; F (1,10) = 2.53, p: 0.142.	Spatial Problem: F (4,40) = 0.28, p: 0.891. SP x Genotype; F (4.40) = 2.21, p: 0.085. **Genotype; F(1,10) = 7.11, p: 0.024.**

Abbreviations. Nobj: Novel Object; OF: Open Field; SP: Spatial Problem; F: Female; M: Male.
Highlighted in bold and underlined are significant effects.

ATF1 and ICER, or levels of CREB protein, but did result in the loss of CREB phosphorylation at S133 when assessed at the level of individual CA1 neurons, and in western blots of hippocampal slices. We also observed an unexpected difference in the extent of DAPI staining in the nuclei of CA1 pyramidal neurons between control mice and CREB S133A mice, with fewer DAPI-stained pixels in the nuclei of CREB S133A mutant CA1 neurons. Since DAPI binds and stains DNA, assertions as to the size of the nucleus *per se* cannot be robustly made. However, it may

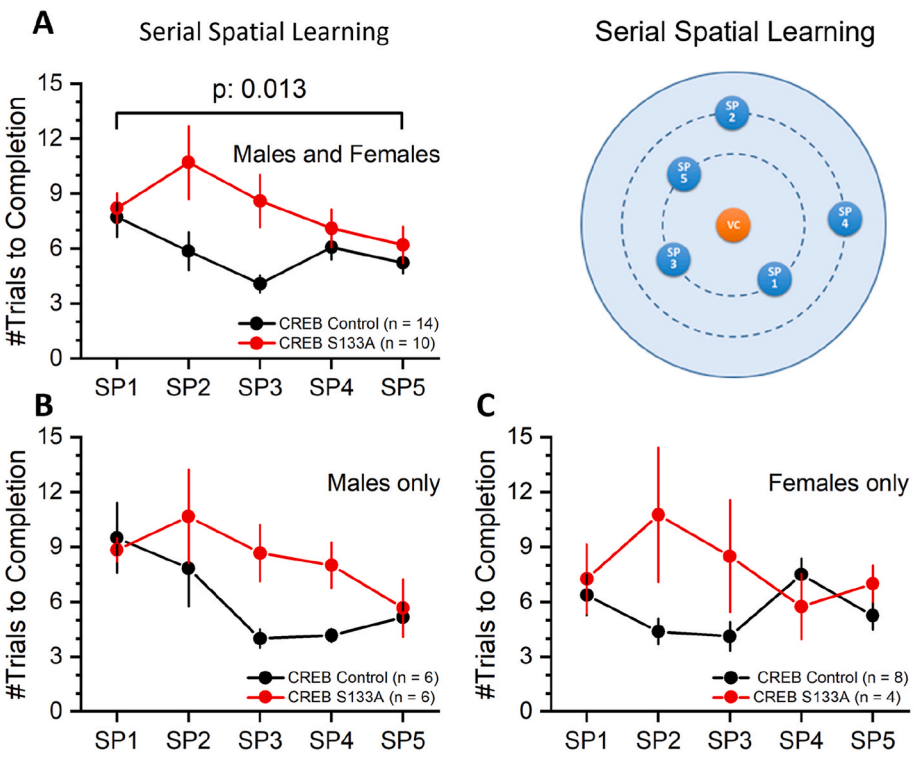

Fig. 3. Intact spatial reference memory, but deficient spatial cognitive flexibility in CREB S133A mutant mice. A) Despite similar levels of performance on first exposure to the spatial learning task, subsequent performance on the serial spatial learning version of the water maze was impaired in CREB S133A mice (red symbols and lines; $F_{1,20} = 7.40$, p: 0.013). The performance of males and females of both genotypes across these spatial tasks is shown in panels B and C, respectively. The inset shows the five sequential locations of the platform used in the test (SP1 – SP5) and the location of the platform for the visually-cued (VC) assessment of gross sensory and motor function. Data are presented as mean ± SEM. Further statistical analysis is provided in Table 2.

be possible that the loss of activity-dependent, CREB-mediated nuclear signalling in the CREB S133A mutant could affect nuclear morphology (Mozolewski et al., 2021) leading to a shrinking of the nuclear envelope and hence a smaller area of DAPI staining. Alternatively, the absence of a CREB S133-dependent transcriptional stimulus may alter the structure of DNA and hence potentially restrict binding of DAPI, leading to an apparent decrease in nucleus size. Since we are not aware of a similar level of interrogation of DAPI staining or nuclear morphology in previous CREB mutants, or others for that matter, the explanation for this peculiar observation is presently elusive.

With this CREB S133A mutant mouse, although not providing a full characterization of all the possible roles CREB S133 may play, we have assessed the role of CREB S133A in hippocampal synaptic activity and in tests of locomotion, neophobia, anxiety-like behaviour and hippocampus-dependent learning and memory. Through this series of studies we have been able to determine the role of CREB S133 in neuronal function, in terms of its influence on basal synaptic transmission and long-term potentiation, and in an assay of learning and memory – the serial spatial learning task.

Our observations, in both the Nestin-Cre and CaMKIIα-Cre CREB S133A mutant mice, are at odds with negative findings based on a constitutive CREB S133A mutant mouse (Briand et al., 2015). Notably in that study the authors precluded a role for CREB S133 in CREB-mediated gene transcription under basal conditions and in response to fear conditioning, and in two forms of hippocampus- and striatum-dependent learning and memory, whereas we have observed a requirement for CREB S133 in gene transcription in neurons (Wingate et al., 2009; Hunter et al., 2017), macrophages (Elcombe et al., 2013) and fibroblasts (Naqvi et al., 2014). The authors speculated that other forms of CREB regulation are more important in regulating CREB-dependent processes such as glycosylation, phosphorylation at S142 or CREB-regulated transcriptional coactivators (CRTCs). It is possible that these mechanisms do come to dominate in response to the constitutive loss of S133, and the role of S133 may only be appreciated using the conditional temporally- and spatially-restricted approach associated with the use of a promoter for the postnatally-expressed CaMKIIα, as we have done here. Accordingly, and in contrast, our observations give strong support to the importance of the phosphorylation of CREB S133 for at least some aspects of neuronal and cognitive function in the mammalian brain.

A spate of papers in the early 1990s (Dash et al., 1990; Kaang et al., 1993; Alberini et al., 1994; Bourtchuladze et al., 1994; Yin et al., 1994) implicated CREB as a key factor in learning and memory in *Aplysia*, *Drosophila* and mammals. The original CREB mouse mutant had a deletion of two (α/δ) of three CREB isoforms and an up-regulation of the remaining β isoform (Bourtchuladze et al., 1994). This mouse, used as a positive control in the constitutive S133A mutant study (Briand et al., 2015), displayed deficits in fear conditioning and the water maze, and displayed a decrementing LTP that returned to baseline within 90 min of LTP induction. Subsequent mouse mutants of CREB yielded conflicting results as to the role of CREB in synaptic plasticity and learning and memory (Gass et al., 1998; Pittenger et al., 2002; Balschun et al., 2003), which may be attributable at least in part to compensation by transcription factors related to CREB, subtleties as to experimental protocols, or in the background strains of mice (Barco and Marie, 2011; Kida and Serita, 2014). More consistent observations have been made with gain of function CREB mutants which provoke enhanced synaptic plasticity and learning and memory (Barco and Marie, 2011; Kida and Serita, 2014). These observations provide the rationale for therapeutic strategies designed to increase the activity of CREB via the inhibition of phosphodiesterases, allowing greater activation of cyclic mononucleotide-dependent CREB S133 kinases such as PKA, and through which such inhibitors are believed to exert their cognition- and plasticity-enhancing effects across the lifespan and in neurodegenerative conditions (Puzzo et al., 2009; Palmeri et al., 2013; Bollen et al., 2014; Heckman et al., 2015; Teich et al., 2015; Yanai and Endo, 2019; Zuccarello et al., 2020).

Our observations, in a conditional, forebrain-specific and post-natal CREB S133A mutant mouse, support the importance of CREB S133 in regulating synaptic transmission, long-term potentiation and some forms of cognition. Having confirmed the loss of CREB S133 in hippocampal area CA1 (Fig. 1), we demonstrated that the CREB mutant did not display impairments in locomotor/exploratory behaviour or the

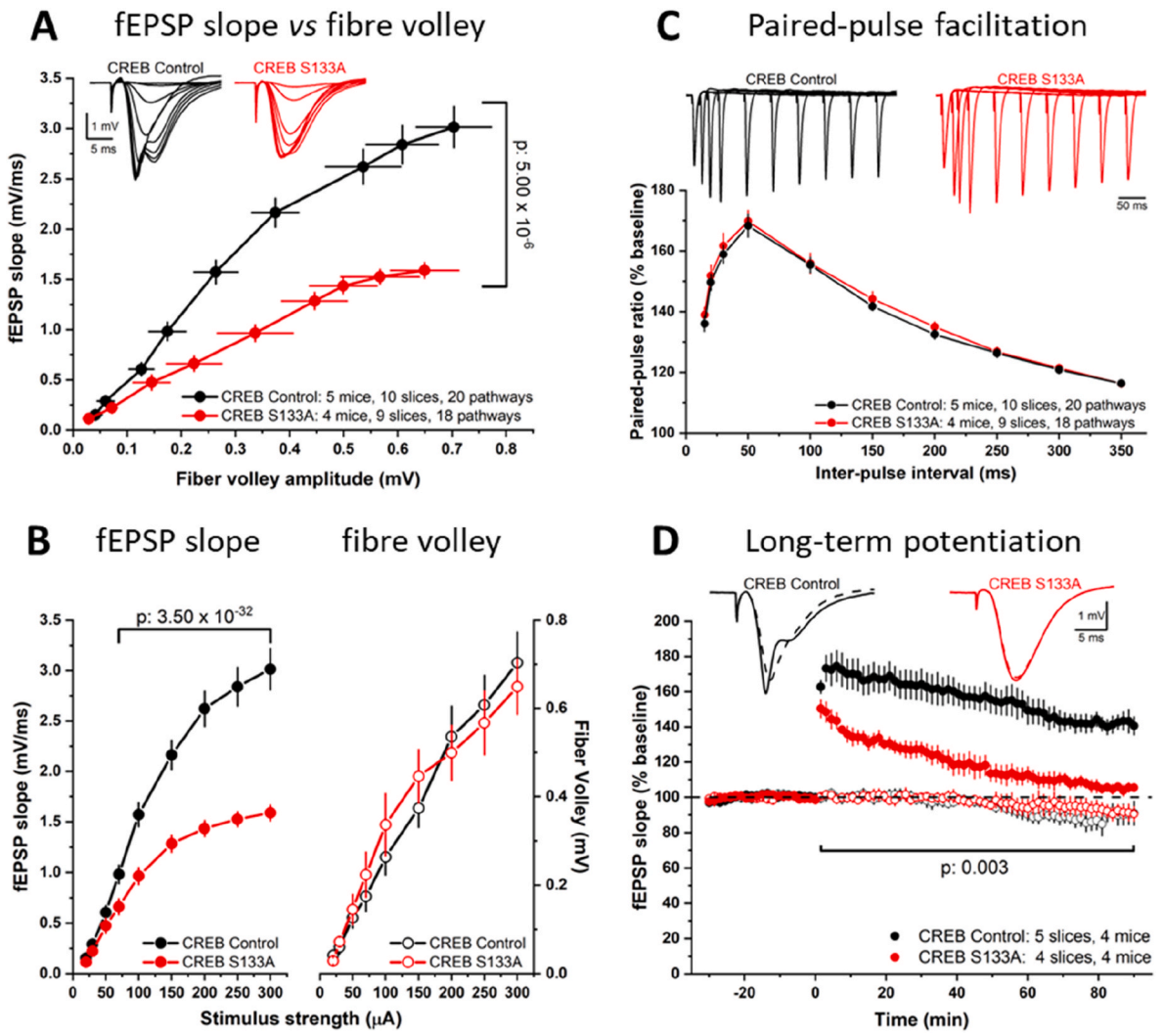

Fig. 4. CREB S133 regulates basal synaptic transmission and is necessary for LTP. A) CREB S133A mice (red lines and symbols) showed an impairment in basal synaptic transmission compared to CREB Control mice (black lines and symbols) when the fEPSP slope is plotted as a function of the presynaptic fibre volley evoked at each stimulus intensity ($F_{1,36} = 28.82$, p: 5.00×10^{-6}). Inset are representative CA1 fEPSPs in hippocampal slices from CREB Control (left, black) and CREB S133A mice (right, red). B) An analysis of fEPSP slope as a function of stimulus strength (left panel; filled symbols) showed a deficit in basal synaptic transmission in hippocampal slices from CREB S133A mice compared to CREB Control mice. A simple main effects analysis of genotype x stimulus strength revealed a significant difference in fEPSP slopes between genotypes starting at 70 μA ($F_{8,288} = 28.13$, p: 3.50×10^{-32}), but not in the presynaptic fibre volley amplitudes (right panel; open symbols; data from 12 to 13 slices in which the fiber volley could be clearly discerned in Control and CREB S133A slices, respectively). C) No difference in paired-pulse facilitation was seen between the two genotypes ($F_{1,36} = 0.29$, p: 0.590) indicative of similar probabilities of glutamate release between the two groups. D) Mice lacking CREB S133 show a pronounced impairment in TBS-induced LTP when measured over the 90 min of the recording after the induction of LTP at t = 0 ($t_{6.02} = 4.70$, p: 0.003). Open symbols refer to the simultaneously-recorded control (non-TBS) pathway. Inset are representative fEPSPs from CREB Control (black, left) and CREB S133A slices (red, right) taken 15 min before (dashed lines) and 80 min after the induction of LTP (solid lines). Data are presented as mean ± SEM.

response to novelty (Fig. 2A), an anxiety-like phenotype (Fig. 2B), nor a deficit in spatial working memory (Fig. 2C) or simple spatial learning in which mice had to locate a submerged platform (SP1; Fig. 3). Instead, the CREB S133A mutant was impaired on a serial spatial learning task in which several new platform locations must be learned (Chen et al., 2000; Daumas et al., 2017) (Fig. 3).

This task is a measure of memory retention, in being able to remember the location of a platform, and cognitive flexibility in being able to promptly update the relevant spatial reference memory to the new location. The impairment in the CREB mutant indicates the importance of CREB S133 for this form of cognition. It should be noted, however, that performance was similar between the mutant and the control mice during SP1, SP4 and SP5. For the first exposure to the task, it is possible that, in the absence of any prior confounding platform locations, sufficient training to the initial platform location (up to 6 trials per day with ~4 min inter-trial interval) may recruit CREB S133-independent forms of learning. Indeed, intensive training overcame the water maze spatial reference memory deficit in the original CREB α/δ mutant (Bourtchuladze et al., 1994). In contrast, acquiring subsequent locations SP2 and SP3 may have been compromised through interference with the memory of the prior locations, suggesting a role for CREB S133 in allowing the cognitive flexibility necessary for spatial discrimination. The similar performance in the last two locations (SP 4 and SP5) between mutants and control mice suggests that with repeated training, forms of learning independent of CREB S133 were being recruited. These could involve other phosphorylation sites on CREB, cAMP-regulated transcriptional coactivator (CRTC)-mediated regulation of CREB (Barco and Marie, 2011; Belgacem and Borodinsky, 2017) or indeed additional plasticity-related transcription factors (Nonaka et al., 2014).

A potential basis for this deficit resides in the observations we made at the cellular level of impaired basal synaptic transmission and a deficit

in LTP, albeit in slices from male mice, but likely to be true for female mice given their similar behaviour across a range of assays. In contrast to the original constitutive CREB α/δ mutant, which had *increased* basal synaptic transmission (Bourtchuladze et al., 1994), the CREB S133A mutant had a clear impairment (Fig. 4A and B). This difference may be due to the constitutive nature of the original CREB α/δ mutation, and potentially the increased expression of the β isoform. However, this deficit in synaptic transmission, which was not due to an impairment in the probability of glutamate release (Fig. 4C), but more likely a deficit in the expression or trafficking of glutamate AMPA receptors, in itself is unlikely to be an explanation for the impairment in the serial spatial learning task since a mouse mutant for a CREB S133 kinase, MSK1, also displayed impaired basal synaptic transmission, but no deficit in serial spatial learning, which was paralleled by intact LTP (Daumas et al., 2017). Instead, and in contrast, the cognitive deficit in the CREB S133A mutant likely resides in an impairment in the ability of synapses to undergo experience-dependent modifications of synaptic strength, and is exemplified in this study via the pronounced LTP deficit in the CREB S133A mutant (Fig. 4D). Such an impairment in a form of hippocampal synaptic plasticity considered to a cornerstone of learning and memory (Morris, 2006) may be expected to have a greater impact on spatial learning than those observed in the serial spatial learning task. One possibility is that the plasticity that remains in the CREB S133A mutant, coupled with the intensive training on the test, is sufficient to overcome the plasticity deficit. However, memory for subsequent platform locations and the ability to switch to a new location may require the intact LTP seen in the controls. Ultimately, familiarity with the test through repeated exposure may recruit non CREB S133-dependent strategies. Thus, the involvement of CREB S133 in learning and memory may be carefully titrated against both the intensity of the training or experience, and the extent of exposure to it.

The LTP deficit in the CREB S133A mutant shares striking similarities with the LTP deficit in the original CREB α/δ null mutant (Bourtchuladze et al., 1994). LTP in both, albeit induced by different stimulation parameters and recording configurations (TBS and interface slice vs. tetanus and submerged slice, respectively), decayed to baseline within ~90 min. This decay of LTP is similar to that caused by the inhibitor of transcription, actinomycin D, under the current experimental conditions (Daumas et al., 2017), and suggests the requirement for CREB S133-dependent transcription for the induction and maintenance of LTP. This suggestion is supported by work with the constitutively-active VP16 CREB mutant in which LTP induction is facilitated, yet insensitive to actinomycin D (Barco et al., 2002), and in a gain-of-function mutant (CREB Y134F) in which the affinity for PKA is increased and LTP is augmented (Suzuki et al., 2011). In both these mutants cognition was affected, with evidence of both enhanced (Suzuki et al., 2011) and impaired (Viosca et al., 2009) cognitive function, suggestive of a need for careful regulation of CREB-dependent gene expression.

These observations point to the importance of the phosphorylation of CREB S133 as vital for the regulation of synaptic transmission, LTP and spatial cognitive flexibility. Additional studies are required to establish whether other forms of synaptic plasticity and cognition are impaired, and indeed the gene expression profiles regulated under these conditions. This is especially important as the phosphorylation of CREB at S133 is only one of several means by which CREB is regulated, for example via phosphorylation of S142 and S143, or phosphorylation-independent CRTCs (Barco and Marie, 2011; Belgacem and Borodinsky, 2017). Such studies will be of value given the medicinal chemistry efforts targeting CREB for the remediation of a variety of congenital, acquired, and age-related impairments of cognition.

CRediT authorship contribution statement

Lorenzo Morè: Formal analysis, Investigation, Data curation, Writing – review & editing, Visualization. **Lucia Privitera:** Investigation, Writing – review & editing, Visualization. **Philippa Perrett:** Investigation, Visualization. **Daniel D. Cooper:** Software, Investigation, Visualization. **Manuel Van Gijsel Bonnello:** Investigation. **J. Simon C. Arthur:** Methodology, Resources, Writing – review & editing. **Bruno G. Frenguelli:** Conceptualization, Data curation, Writing – original draft, Visualization, Supervision, Project administration, Funding acquisition.

Declaration of competing interest

BGF is the Editor-in-Chief of *Neuropharmacology*.

Data availability

Data will be made available on request.

Acknowledgements

We thank the BBSRC (BB/L00139X/1 to BGF, and Doctoral Support BB/M01116X/1 to DDC and PP), WPH Charitable Trust, the Sylvia Waddilove Foundation and the School of Life Sciences pump-priming fund for financial support. We are grateful to Dr Stefania Fasano and Prof Riccardo Brambilla (San Raffaele Scientific Institute, Milan, Italy) for providing the Tg(Camk2a-cre)159Kln CRE recombinase mouse (MGI:2176753), and to the staff of the Biomedical Services Units, Universities of Warwick and Dundee for their excellent animal husbandry.

Appendix A. Supplementary data

Supplementary data to this article can be found online at https://doi.org/10.1016/j.neuropharm.2022.109237.

References

Alberini, C.M., Ghirardi, M., Metz, R., Kandel, E.R., 1994. C/EBP is an immediate-early gene required for the consolidation of long-term facilitation in Aplysia. Cell 76, 1099–1114.
Alberini, C.M., Kandel, E.R., 2014. The regulation of transcription in memory consolidation. Cold Spring Harbor Perspect. Biol. 7, a021741.
Balschun, D., Wolfer, D.P., Gass, P., Mantamadiotis, T., Welzl, H., Schutz, G., Frey, J.U., Lipp, H.P., 2003. Does cAMP response element-binding protein have a pivotal role in hippocampal synaptic plasticity and hippocampus-dependent memory? J. Neurosci. 23, 6304–6314.
Barco, A., Alarcon, J.M., Kandel, E.R., 2002. Expression of constitutively active CREB protein facilitates the late phase of long-term potentiation by enhancing synaptic capture. Cell 108, 689–703.
Barco, A., Marie, H., 2011. Genetic approaches to investigate the role of CREB in neuronal plasticity and memory. Mol. Neurobiol. 44, 330–349.
Belgacem, Y.H., Borodinsky, L.N., 2017. CREB at the crossroads of activity-dependent regulation of nervous system development and function. Adv. Exp. Med. Biol. 1015, 19–39.
Bianchi, V., Gambino, F., Muzio, L., Toniolo, D., Humeau, Y., D'Adamo, P., 2012. Forebrain deletion of alphaGDI in adult mice worsens the pre-synaptic deficit at cortico-lateral amygdala synaptic connections. PLoS One 7, e29763.
Bollen, E., Puzzo, D., Rutten, K., Privitera, L., De Vry, J., Vanmierlo, T., Kenis, G., Palmeri, A., D'Hooge, R., Balschun, D., Steinbusch, H.M., Blokland, A., Prickaerts, J., 2014. Improved long-term memory via enhancing cGMP-PKG signaling requires cAMP-PKA signaling. Neuropsychopharmacology 39, 2497–2505.
Bourtchuladze, R., Frenguelli, B., Blendy, J., Cioffi, D., Schutz, G., Silva, A.J., 1994. Deficient long-term memory in mice with a targeted mutation of the cAMP-responsive element-binding protein. Cell 79, 59–68.
Briand, L.A., Lee, B.G., Lelay, J., Kaestner, K.H., Blendy, J.A., 2015. Serine 133 phosphorylation is not required for hippocampal CREB-mediated transcription and behavior. Learn. Mem. 22, 109–115.
Chen, G., Chen, K.S., Knox, J., Inglis, J., Bernard, A., Martin, S.J., Justice, A., McConlogue, L., Games, D., Freedman, S.B., Morris, R.G., 2000. A learning deficit related to age and beta-amyloid plaques in a mouse model of Alzheimer's disease. Nature 408, 975–979.
D'Adamo, P., Masetti, M., Bianchi, V., Morè, L., Mignogna, M.L., Giannandrea, M., Gatti, S., 2014. RAB GTPases and RAB-interacting proteins and their role in the control of cognitive functions. Neurosci. Biobehav. Rev. 46 Pt 2, 302–314.
Dash, P.K., Hochner, B., Kandel, E.R., 1990. Injection of the cAMP-responsive element into the nucleus of Aplysia sensory neurons blocks long-term facilitation. Nature 345, 718–721.
Daumas, S., Hunter, C.J., Mistry, R.B., More, L., Privitera, L., Cooper, D.D., Reyskens, K. M., Flynn, H.T., Morris, R.G., Arthur, J.S., Frenguelli, B.G., 2017. The kinase function of MSK1 regulates BDNF signaling to CREB and basal synaptic transmission,

but is not required for hippocampal long-term potentiation or spatial memory. eNeuro 4.
Di Domenico, M., Jokwitz, M., Witke, W., Pilo Boyl, P., 2021. Specificity and redundancy of profilin 1 and 2 function in brain development and neuronal structure. Cells 10.
Elcombe, S.E., Naqvi, S., Van Den Bosch, M.W., MacKenzie, K.F., Cianfanelli, F., Brown, G.D., Arthur, J.S., 2013. Dectin-1 regulates IL-10 production via a MSK1/2 and CREB dependent pathway and promotes the induction of regulatory macrophage markers. PLoS One 8, e60086.
Flavell, S.W., Greenberg, M.E., 2008. Signaling mechanisms linking neuronal activity to gene expression and plasticity of the nervous system. Annu. Rev. Neurosci. 31, 563–590.
Gass, P., Wolfer, D.P., Balschun, D., Rudolph, D., Frey, U., Lipp, H.P., Schutz, G., 1998. Deficits in memory tasks of mice with CREB mutations depend on gene dosage. Learn. Mem. 5, 274–288.
Heckman, P.R., Wouters, C., Prickaerts, J., 2015. Phosphodiesterase inhibitors as a target for cognition enhancement in aging and Alzheimer's disease: a translational overview. Curr. Pharmaceut. Des. 21, 317–331.
Hunter, C.J., Remenyi, J., Correa, S.A., Privitera, L., Reyskens, K., Martin, K.J., Toth, R., Frenguelli, B.G., Arthur, J.S.C., 2017. MSK1 regulates transcriptional induction of Arc/Arg3.1 in response to neurotrophins. FEBS Open Bio 7, 821–834.
Johannessen, M., Delghandi, M.P., Moens, U., 2004. What turns CREB on? Cell. Signal. 16, 1211–1227.
Kaang, B.K., Kandel, E.R., Grant, S.G., 1993. Activation of cAMP-responsive genes by stimuli that produce long-term facilitation in Aplysia sensory neurons. Neuron 10, 427–435.
Kaneko, K., Xu, P., Cordonier, E.L., Chen, S.S., Ng, A., Xu, Y., Morozov, A., Fukuda, M., 2016. Neuronal Rap1 regulates energy balance, glucose homeostasis, and leptin actions. Cell Rep. 16, 3003–3015.
Kida, S., Serita, T., 2014. Functional roles of CREB as a positive regulator in the formation and enhancement of memory. Brain Res. Bull. 105, 17–24.
Lisman, J., Cooper, K., Sehgal, M., Silva, A.J., 2018. Memory formation depends on both synapse-specific modifications of synaptic strength and cell-specific increases in excitability. Nat. Neurosci. 21, 309–314.
Mao, F., Wang, H., Ni, W., Zheng, X., Wang, M., Bao, K., Ling, D., Li, X., Xu, Y., Zhang, H., Li, J., 2018. Design, synthesis, and biological evaluation of orally available first-generation dual-target selective inhibitors of acetylcholinesterase (AChE) and phosphodiesterase 5 (PDE5) for the treatment of Alzheimer's disease. ACS Chem. Neurosci. 9, 328–345.
Minichiello, L., Korte, M., Wolfer, D., Kuhn, R., Unsicker, K., Cestari, V., Rossi-Arnaud, C., Lipp, H.P., Bonhoeffer, T., Klein, R., 1999. Essential role for TrkB receptors in hippocampus-mediated learning. Neuron 24, 401–414.
Morè, L., Gravius, A., Pietraszek, M., Belozertseva, I., Malyshkin, A., Shekunova, E., Barberi, C., Schaefer, D., Schmidt, W.J., Danysz, W., 2007. Comparison of the mGluR1 antagonist A-841720 in rat models of pain and cognition. Behav. Pharmacol. 18, 273–281.
Morris, R.G., 2006. Elements of a neurobiological theory of hippocampal function: the role of synaptic plasticity, synaptic tagging and schemas. Eur. J. Neurosci. 23, 2829–2846.
Mozolewski, P., Jeziorek, M., Schuster, C.M., Bading, H., Frost, B., Dobrowolski, R., 2021. The role of nuclear Ca2+ in maintaining neuronal homeostasis and brain health. J. Cell Sci. 134.
Naqvi, S., Martin, K.J., Arthur, J.S., 2014. CREB phosphorylation at Ser133 regulates transcription via distinct mechanisms downstream of cAMP and MAPK signaling. Biochem. J. 458, 469–479.
Ni, W., Wang, H., Li, X., Zheng, X., Wang, M., Zhang, J., Gong, Q., Ling, D., Mao, F., Zhang, H., Li, J., 2018. Novel tadalafil derivatives ameliorates scopolamine-induced cognitive impairment in mice via inhibition of acetylcholinesterase (AChE) and phosphodiesterase 5 (PDE5). ACS Chem. Neurosci. 9, 1625–1636.
Nonaka, M., Kim, R., Sharry, S., Matsushima, A., Takemoto-Kimura, S., Bito, H., 2014. Towards a better understanding of cognitive behaviors regulated by gene expression downstream of activity-dependent transcription factors. Neurobiol. Learn. Mem. 115, 21–29.
Oettinghaus, B., Schulz, J.M., Restelli, L.M., Licci, M., Savoia, C., Schmidt, A., Schmitt, K., Grimm, A., Morè, L., Hench, J., Tolnay, M., Eckert, A., D'Adamo, P., Franken, P., Ishihara, N., Mihara, K., Bischofberger, J., Scorrano, L., Frank, S., 2016. Synaptic dysfunction, memory deficits and hippocampal atrophy due to ablation of mitochondrial fission in adult forebrain neurons. Cell Death Differ. 23, 18–28.
Palmeri, A., Privitera, L., Giunta, S., Loreto, C., Puzzo, D., 2013. Inhibition of phosphodiesterase-5 rescues age-related impairment of synaptic plasticity and memory. Behav. Brain Res. 240, 11–20.
Pennucci, R., Talpo, F., Astro, V., Montinaro, V., Morè, L., Cursi, M., Castoldi, V., Chiaretti, S., Bianchi, V., Marenna, S., Cambiaghi, M., Tonoli, D., Leocani, L., Biella, G., D'Adamo, P., de Curtis, I., 2016. Loss of either Rac1 or Rac3 GTPase differentially affects the behavior of mutant mice and the development of functional GABAergic networks. Cerebr. Cortex 26, 873–890.
Pittenger, C., Huang, Y.Y., Paletzki, R.F., Bourtchouladze, R., Scanlin, H., Vronskaya, S., Kandel, E.R., 2002. Reversible inhibition of CREB/ATF transcription factors in region CA1 of the dorsal hippocampus disrupts hippocampus-dependent spatial memory. Neuron 34, 447–462.
Privitera, L., More, L., Cooper, D.D., Richardson, P., Tsogka, M., Hebenstreit, D., Arthur, J.S.C., Frenguelli, B.G., 2020. Experience recruits MSK1 to expand the dynamic range of synapses and enhance cognition. J. Neurosci. 40, 4644–4660.
Puzzo, D., Staniszewski, A., Deng, S.X., Privitera, L., Leznik, E., Liu, S., Zhang, H., Feng, Y., Palmeri, A., Landry, D.W., Arancio, O., 2009. Phosphodiesterase 5 inhibition improves synaptic function, memory, and amyloid-beta load in an Alzheimer's disease mouse model. J. Neurosci. 29, 8075–8086.
Reyskens, K.M., Arthur, J.S., 2016. Emerging roles of the mitogen and stress activated kinases MSK1 and MSK2. Front. Cell Dev. Biol. 4, 56.
Rios, M., Fan, G., Fekete, C., Kelly, J., Bates, B., Kuehn, R., Lechan, R.M., Jaenisch, R., 2001. Conditional deletion of brain-derived neurotrophic factor in the postnatal brain leads to obesity and hyperactivity. Mol. Endocrinol. 15, 1748–1757.
Stilling, R.M., Ronicke, R., Benito, E., Urbanke, H., Capece, V., Burkhardt, S., Bahari-Javan, S., Barth, J., Sananbenesi, F., Schutz, A.L., Dyczkowski, J., Martinez-Hernandez, A., Kerimoglu, C., Dent, S.Y., Bonn, S., Reymann, K.G., Fischer, A., 2014. K-Lysine acetyltransferase 2a regulates a hippocampal gene expression network linked to memory formation. EMBO J. 33, 1912–1927.
Suzuki, A., Fukushima, H., Mukawa, T., Toyoda, H., Wu, L.J., Zhao, M.G., Xu, H., Shang, Y., Endoh, K., Iwamoto, T., Mamiya, N., Okano, E., Hasegawa, S., Mercaldo, V., Zhang, Y., Maeda, R., Ohta, M., Josselyn, S.A., Zhuo, M., Kida, S., 2011. Upregulation of CREB-mediated transcription enhances both short- and long-term memory. J. Neurosci. 31, 8786–8802.
Teich, A.F., Nicholls, R.E., Puzzo, D., Fiorito, J., Purgatorio, R., Fa, M., Arancio, O., 2015. Synaptic therapy in Alzheimer's disease: a CREB-centric approach. Neurotherapeutics 12, 29–41.
Tolson, K.P., Gemelli, T., Gautron, L., Elmquist, J.K., Zinn, A.R., Kublaoui, B.M., 2010. Postnatal Sim1 deficiency causes hyperphagic obesity and reduced Mc4r and oxytocin expression. J. Neurosci. 30, 3803–3812.
Viosca, J., Malleret, G., Bourtchouladze, R., Benito, E., Vronskava, S., Kandel, E.R., Barco, A., 2009. Chronic enhancement of CREB activity in the hippocampus interferes with the retrieval of spatial information. Learn. Mem. 16, 198–209.
Wickham, R.J., Alexander, J.M., Eden, L.W., Valencia-Yang, M., Llamas, J., Aubrey, J.R., Jacob, M.H., 2019. Learning impairments and molecular changes in the brain caused by β-catenin loss. Hum. Mol. Genet. 28, 2965–2975.
Wingate, A.D., Martin, K.J., Hunter, C., Carr, J.M., Clacher, C., Arthur, J.S., 2009. Generation of a conditional CREB Ser133Ala knockin mouse. Genesis 47, 688–696.
Wolf, L.W., LaRegina, M.C., Tolbert, D.L., 1996. A behavioral study of the development of hereditary cerebellar ataxia in the shaker rat mutant. Behav. Brain Res. 75, 67–81.
Yanai, S., Endo, S., 2019. PDE3 inhibitors repurposed as treatments for age-related cognitive impairment. Mol. Neurobiol. 56, 4306–4316.
Yin, J.C., Wallach, J.S., Del, V.M., Wilder, E.L., Zhou, H., Quinn, W.G., Tully, T., 1994. Induction of a dominant negative CREB transgene specifically blocks long-term memory in Drosophila. Cell 79, 49–58.
Zuccarello, E., Acquarone, E., Calcagno, E., Argyrousi, E.K., Deng, S.X., Landry, D.W., Arancio, O., Fiorito, J., 2020. Development of novel phosphodiesterase 5 inhibitors for the therapy of Alzheimer's disease. Biochem. Pharmacol. 176, 113818.